PHYSICAL REVIEW A VOLUME 26, NUMBER 1 JULY 1982

Extracavity laser band-shape and bandwidth modification

D. S. Elliott, Rajarshi Roy, and S. J. Smith*
Joint Institute for Laboratory Astrophysics, University of Colorado and National Bureau of Standards, Boulder, Colorado 80309
(Received 15 December 1981)

A technique for modifying the laser power spectrum by use of an acousto-optic modulator is described. The theory of the power spectrum resulting from frequency modulation by Gaussian noise is reviewed, and several examples of broadened laser power spectra are presented.

I. INTRODUCTION

We have developed a method of controlled modification of the bandwidth and band shape of a cw laser power spectrum by superimposing frequency fluctuations onto a laser beam. This broadening process is completely external to the cavity, so the method is applicable to laser beams with no modifications to the laser itself. This is the first development of a device for extending bandwidth and modifying band shape of an external narrowband laser beam in a statistically defined way. In principle, it provides a means for obtaining arbitrarily wide band, yet single-mode laser beams.

Bandwidth and band-shape control of the laser power spectrum are attractive for several reasons. Our direct interest in developing this technology is for the study of the influence of laser frequency fluctuations on a strong transition in a two-level atom. This problem has received considerable attention from theorists (see Refs. 1 and 2, for example, and references contained therein), but very little experimental study has been undertaken.[3] With the technique described in this report, we can vary both the magnitude of the frequency fluctuations, and the rapidity with which they occur, thus providing a versatile method of studying such a nonlinear atomic system.

Other potential applications of this method can be found in the study of laser-atom interactions which do not involve the hyperfine structure of the atom, and in the efficient excitation of inhomogeneously broadened transitions. Using this technique, the laser spectrum can be made broader than the hyperfine splitting, eliminating its effects. In the second case, excitation of an entire sample of atoms or molecules can be attained using this technique when the transition is inhomogeneously broadened. Thus, instead of saturating the transition for only one subgroup, the laser spectrum may be broadened to be in resonance with all the atoms or molecules in the sample.

The basic functions necessary for superimposing frequency fluctuations on the laser are provided by a noise module, a voltage controlled oscillator (VCO) and an acousto-optic modulator (AOM). The VCO transforms the voltage fluctuations from the noise module into frequency fluctuations, yielding a constant-amplitude, varying-frequency rf signal, as shown in Fig. 1. This rf is added to the laser frequency by means of the AOM, resulting in a broadened laser power spectrum. The shape of the rf power spectrum is strongly dependent on the power spectrum of the white noise with which the VCO is frequency modulated.

In this report we describe the techniques used for superimposing frequency fluctuations onto the laser beam, discuss the theory of frequency modulation using Gaussian noise, and present the rf and laser power spectra obtained by this method.

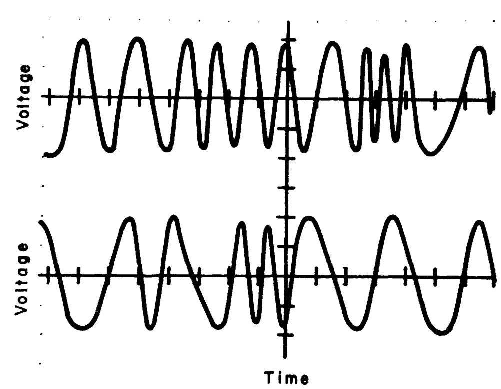

FIG. 1. Examples of the constant amplitude, fluctuating frequency rf signal, corresponding to a root-mean-square deviation frequency of about 40 MHz. The apparent amplitude modulation is due to the limited frequency response of the oscilloscope. The horizontal scale is 2.5 nsec/div.

II. THE SYSTEM

The system used is shown in the block diagram (Fig. 2). The noise module has a flat power spectrum (± 2 dB) from ~ 1 kHz to ~ 400MHz, with the voltage following a Gaussian probability distribution. The ratio of upper- to lower- frequency cutoffs should be greater than 1000 for a well-defined laser bandshape. The output power level is -47 dBm/10 kHz, corresponding to a rms voltage of about 200 mV into a 50-Ω load. The white noise power spectrum cutoff frequency is controlled using a seven- or eight-pole low-pass filter, and the amplitude is controlled by attenuators and/or an amplifier. The 30-dB gain of this white noise amplifier is flat to ± 1 dB over the frequency range 2 kHz$-$400 MHz, and the output power at 1-dB gain compression is $+28$ dBm, 25 dB in excess of the maximum power we ever use to modulate the voltage-controlled oscillator. This high power capability ensures that voltage will not be clipped for excursions less than 18 times the rms voltage.

The voltage controlled oscillator was selected partly for its low input capacitance (~ 45 pf). The 50-Ω impedance of the prototype system and this input capacitance of the VCO define an RC cutoff frequency of the noise power spectrum at about 100 MHz. In addition, the frequency versus input voltage tuning curve must be linear to within a few percent over the range of input voltage fluctuations, and the slope of this tuning curve must be large (~ 100 MHz/V). The output of this oscillator is constant in amplitude, but varying in frequency around 3.3 GHz. The resulting power spectrum will be described in Sec. III.

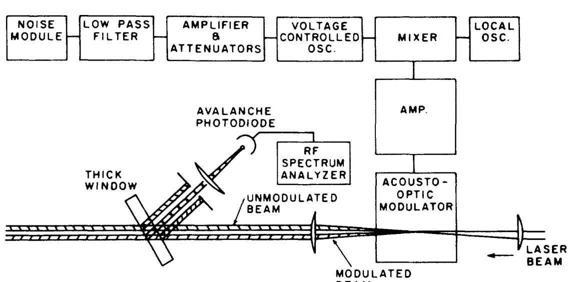

FIG. 2. Block diagram of the electronics and detection scheme. The components which we used are as follows: noise module—Micronetics Model 100 MSD-2LEE (modified); noise amplifer—Avantek Model AV-8; voltage controlled oscillator—Avantek Model VTO-8360; mixer—Vari-L Model DBM1200; local oscillator—Avantek Model VTO-8240; RF amplifier—Amplifier Research Model 4W 1000; acousto-optic modulator—Isomet Model 1250-C. Listing of the products is for information transfer purposes and should not be construed as an endorsement by the authors.

The 3.3-GHz output of the VCO beats against the 3.5-GHz local oscillator in a doubly balanced mixer, and the difference frequency signal is amplified to about 1 W. This provides the rf signal required by the acousto-optic modulator that superimposes the rf power spectrum onto the laser beam. An essential property of the modulator is its fast response time (~ 10 nsec).

III. POWER SPECTRUM OF FREQUENCY MODULATION USING GAUSSIAN NOISE

An understanding of the rf power spectrum obtained by frequency modulation using Gaussian noise is essential to a full appreciation of the possibilities for superimposing controlled frequency fluctuations on a laser beam. This problem was first worked out by Middleton,[4,5] and applied to a rectangular noise power spectrum by Stewart.[6] The following discussion presents the theory and solutions for the current application.

The output signal of the oscillator is of the form

$$V_F(t)=A_0\exp\{i[\omega_0 t+\phi(t)]\}\ , \tag{1}$$

where $\phi(t)=2\pi\int_0^t DV(t')\,dt'$ is a Gaussian process since $V(t')$ is a Gaussian process. D is the slope of the tuning curve of the oscillator, and ω_0 is the central frequency of oscillation. The product $DV_{\rm rms}$ describes the rms deviation frequency. In order to determine the power spectrum, we must first consider the autocorrelation function; we make no distinction between the autocorrelation function and the autocovariance function since $V_F(t)$ is an ergodic process (the time averages and ensemble averages are equal).[5] The autocorrelation function is

$$\begin{aligned}R_F(\tau)&=\tfrac{1}{2}\,\mathrm{Re}\lim_{T\to\infty}\frac{1}{T}\int_{-T/2}^{T/2}V_F(t)V_F^*(t+\tau)\,dt\\&=\tfrac{1}{2}\langle V_F(t)V_F^*(t+\tau)\rangle\\&=\frac{A_0^2}{2}\mathrm{Re}\exp(-i\omega_0\tau)\langle\exp\{i[\phi(t)-\phi(t+\tau)]\}\rangle \qquad (2)\\&=\frac{A_0^2}{2}\cos(\omega_0\tau)\exp\{-\tfrac{1}{2}\langle[\phi(t)-\phi(t+\tau)]^2\rangle\}\ . \qquad (3)\end{aligned}$$

This last step follows from the Gaussian moment theorem,[5] and the procedure is outlined in Appendix A.

We are now in a position to apply the Wiener-Khintchine Theorem,[5] which relates the power spectrum $W(f)$, and the autocorrelation function $R(t)$, by the Fourier Transform integral:

$$W(f)=4\int_0^\infty R(t)\cos\omega t\,dt$$

and

$$R(t)=\int_0^\infty W(f)\cos\omega t\,df\ .$$

This results in a power spectrum of the form

$$W_F(f)=A_0^2\int_0^\infty d\tau[\cos(\omega_0-\omega)\tau+\cos(\omega_0+\omega)\tau]\times\exp\{-\tfrac{1}{2}\langle[\phi(t)-\phi(t+\tau)]^2\rangle\}\ .$$

The rapidly varying $\cos(\omega_0+\omega)\tau$ term can be ignored when $\omega_0+\omega \gg \omega_0-\omega$. Under this condition, the shape and width of the rf power spectrum is independent of the central frequency ω_0. This means that our power spectrum is not changed by shifting ω_0 from 3.3 GHz to 200 MHz, since we restrict the width to values much less than 200 MHz.

The argument of the exponential function must now be determined for our specific application, namely when ϕ is the time integral of a noisy voltage. Since $V(t)$ is a stationary process, the following relation can be shown:

$$\begin{aligned}\langle[\phi(t)-\phi(t+\tau)]^2\rangle &=(2\pi D)^2\left\langle\left[\int_0^t V(t)dt-\int_0^{t+\tau}V(t)\,dt\right]^2\right\rangle\\ &=(2\pi D)^2\left\langle\left[\int_0^\tau V(t)dt\right]^2\right\rangle\\ &=(2\pi D)^2\int_0^\tau\int_0^\tau\langle V(t_1)V(t_2)\rangle\,dt_1dt_2\\ &=2(2\pi D)^2\int_0^\tau(\tau-t)R_V(t)\,dt\ ,\end{aligned}\tag{4}$$

where $R_V(t)$ is the autocorrelation function of the noise. The final step above is explained in Appendix B.

Applying the Weiner-Khintchine Theorem to the noise power spectrum, we find the rf power spectrum to be

$$W_F(f)=A_0^2\int_0^\infty d\tau\cos(\omega-\omega_0)\tau\exp\left[-(2\pi D)^2\int_0^\infty W_V(f')\int_0^\tau(\tau-t)\cos\omega' t\,dt\,df'\right]\ ,$$

or, reversing the order of integration in the exponential and evaluating the time integral:

$$W_F(\Delta\omega)=\frac{A_0^2}{2\pi}\int_0^\infty d\tau\cos(\Delta\omega\tau)\left[\exp-2(2\pi D)^2\int_0^\infty W_V(\omega')\left[\frac{\sin\omega'\tau/2}{\omega'}\right]^2 d\omega'\right]\tag{5}$$

where $\Delta\omega=\omega-\omega_0$, and $W(\omega)=W(f)/2\pi$ have been used.

We wish now to consider the case of a rectangular input noise power spectrum with a cutoff at frequency B, described by

$$W_V(\omega)=\begin{cases}\dfrac{\langle V^2\rangle}{2\pi B}, & 0<\omega<2\pi B\ .\\ 0, & \omega>2\pi B\end{cases}$$

The rf power spectrum for this rectangular noise power spectrum is of the form

$$W_F(\Delta\omega)=\frac{A_0^2}{2\pi}\int_0^\infty d\tau\cos(\Delta\omega\tau)\exp\left[-\frac{2\pi D^2\langle V^2\rangle\tau}{B}\int_0^{\pi B\tau}\left[\frac{\sin x}{x}\right]^2dx\right]\ .\tag{6}$$

When the ratio of the deviation to cutoff frequencies DV_{rms}/B is large, the exponential is significant for only small $x(=\omega'\tau/2)$, and we can expand $[(\sin x)/x]^2$ and integrate

$$\int_0^{\pi B\tau}\left[\frac{\sin x}{x}\right]^2dx\sim\pi B\tau\ ,$$

where we have kept only the first term.

The rf power spectrum for large DV_{rms}/B is therefore given by

$$\begin{aligned}W_F(\Delta\omega)&=\frac{A_0^2}{2\pi}\int_0^\infty d\tau\cos(\Delta\omega\tau)\exp(-2\pi^2D^2\langle V^2\rangle\tau^2)\\ &=\frac{A_0^2}{2}\frac{1}{(8\pi^3D^2\langle V^2\rangle)^{1/2}}\exp\left[\frac{-(\Delta\omega)^2}{8\pi^2D^2\langle V^2\rangle}\right]\ .\end{aligned}\tag{7}$$

The FWHM for this distribution is found by setting the exponential equal to one half, from which we obtain

$$\Delta_{\mathrm{FWHM}}=2(2\ln 2)^{1/2}DV_{\mathrm{rms}}\sim 2.35DV_{\mathrm{rms}}\ . \qquad (8)$$

This rf power spectrum is Gaussian and independent of the cutoff frequency. The FWHM varies as the noise voltage amplitude. This result is not surprising for in this regime the frequency changes slowly, and the spectrum is the same as the distribution of frequencies. The total power is found by integrating over all frequencies, and is simply $A_0^2/2$, the time-averaged square of the output voltage of the oscillator.

Equation (6) can also be evaluated when the ratio of deviation frequency to cutoff frequency, DV_{rms}/B, is small. In this case, we can approximate the integral

$$\int_0^{\pi B\tau}\left[\frac{\sin x}{x}\right]^2 dx$$

by its asymptotic value of $\pi/2$. Then we get

$$\begin{aligned} W_F(\Delta\omega)&=\frac{A_0^2}{2\pi}\int_0^{\infty} d\tau\cos(\Delta\omega\tau)\exp\left[-\frac{\pi^2D^2\langle V^2\rangle\tau}{B}\right]\\ &=\frac{A_0^2}{2\pi}\frac{\pi^2D^2\langle V^2\rangle/B}{(\pi^2D^2\langle V^2\rangle/B)^2+(\Delta\omega)^2}\ . \end{aligned} \qquad (9)$$

We again evaluate the FWHM by setting

$$\frac{(\pi^2D^2\langle V^2\rangle/B)^2}{(\pi^2D^2\langle V^2\rangle/B)^2+(\Delta\omega)^2}=\frac{1}{2}\ ,$$

resulting in

$$\Delta_{\mathrm{FWHM}}=\pi D^2\langle V^2\rangle/B\ . \qquad (10)$$

The power spectrum in this regime is Lorentzian, and the bandwidth varies as the noise power spectral density rather than the noise amplitude. The total power is again found to be $A_0^2/2$. Because of the high cutoff frequency B, the frequency output of the oscillator fluctuates very rapidly, decreasing the correlation time of the fluctuations. This leads to an exponential autocorrelation function, and therefore to a Lorentzian power spectrum.

It is important to note that theoretically this process does not involve any amplitude modulation, and that this ideal situation is very nearly achieved with the electronic components used.

IV. DISCUSSION

A typical rf power spectrum is shown in Figs. 3(a) and 3(b). The cutoff frequency B of the noise power spectrum, shown in Fig. 3(c), is 90 MHz, and the deviation frequency DV_{rms} is 27 MHz. Also shown is the power spectrum as computed by numerical integration using Eq. (6). The power spectrum has Lorentzian character close to the center, but falls off rapidly like a Gaussian in the wings. A definite shoulder is seen separating these two regimes, corresponding to the cutoff frequency B, of the noise spectrum.

A log-log plot of rf bandwidth versus deviation frequency is shown in Fig. 4 for deviation frequencies in the range 10–40 MHz. For a cutoff frequency of 10 MHz, this plot is seen to have a slope of 1, as expected from Eq. (8) for the FWHM of a

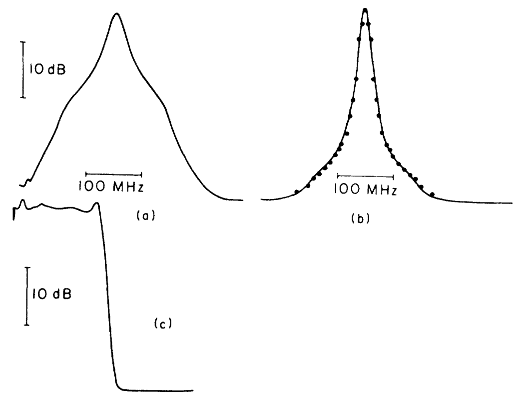

FIG. 3. The observed rf power spectrum, plotted (a) on a logarithmic scale and (b) on a square root scale, resulting from frequency modulation using the noise power spectrum shown in (c), characterized by $B=90$ MHz and $DV_{\mathrm{rms}}=27$ MHz. The dots are results given by numerical integration using Eq. (6).

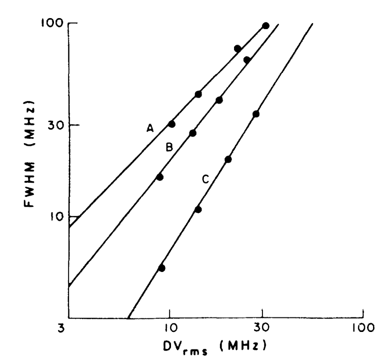

FIG. 4. Log—log plot of rf bandwidth versus the rms deviation frequency. The three lines, A, B, and C, correspond to Gaussian noise cutoff frequencies $B=10$, 27, and 90 MHz, respectively.

Gaussian power spectrum. For $B=28$ MHz and $B=90$ MHz, the slope increases to 1.26 and 1.66, respectively. This again shows that, for deviation frequencies of interest to us, B must be greater than 90 MHz in order to attain a truly Lorentzian power spectrum, for which the slope will be 2 [see Eq. (10)].

Figure 5 shows the laser power spectrum resulting from superimposing the rf power spectrum of Fig. 3 onto a He-Ne laser beam by means of the acousto-optic modulator. The He-Ne laser beam is focused to a beam waist radius of ~ 45 μm, resulting in a response time of ~ 10 nsec. The acousto-optic modulator was positioned so as to exhibit a wide (~ 100 MHz full width) nearly flat dependence of efficiency on frequency. This flat response is crucial for the realization of a well-behaved and useful bandwidth and band-shape control process. The laser power spectrum of Fig. 5 is cut off at about 50 MHz from the central frequency due to the limited frequency response of the acousto-optic modulator defining an upper limit to the useful laser bandwidth obtainable with this device and also to the modulation frequency. The laser power spectrum is determined by beating the broadened modulated laser beam with the unmodulated beam on an avalanche photodiode which has a gain-bandwidth product of 80 GHz. The spectrum, as measured by this method, is almost independent of the linewidth of the laser itself and reflects the true line shape only when the unmodified laser line shape is much narrower than the rf power spectrum. (The laser which we used was determined to have a sub-MHz line width on a millisecond timescale.) The amplitude modulation of the laser beam is measured to be less than 1%.

Figure 6 shows several examples of laser power spectra: with constant B, varying $DV_{\rm rms}$, and vice versa. The change from Gaussian to Lorentzian line shape is evident. Note also the small dependence on B for the two nearly Gaussian lines in Fig. 6(c).

Finally, it should be noted that the theoretical works of Ref. 1 use a model of the laser field for which the correlation function of the laser frequency is described by an exponentially decreasing function of time, in contrast to the $\sin(t)/t$ function produced here. Our system can be modified to the theoretical model by replacing our noise power spectrum, which has a sharp cutoff at angular frequency $2\pi B$ with a Lorentzian noise power spectrum (as produced, for example, by passing white noise through a low-pass RC filter).

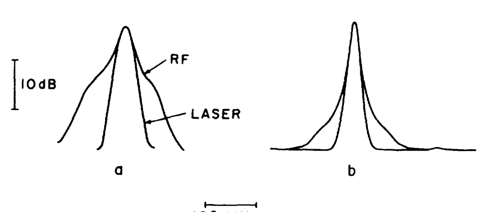

FIG. 5. The rf and laser power spectra for $B=90$ MHz and $DV_{\rm rms}=27$ MHz. The wings of this especially wide rf spectrum are not reproduced in the laser spectrum because of the limited frequency bandwidth of the acousto-optic modulator. (a) and (b) are logarithmic and square root plots, respectively.

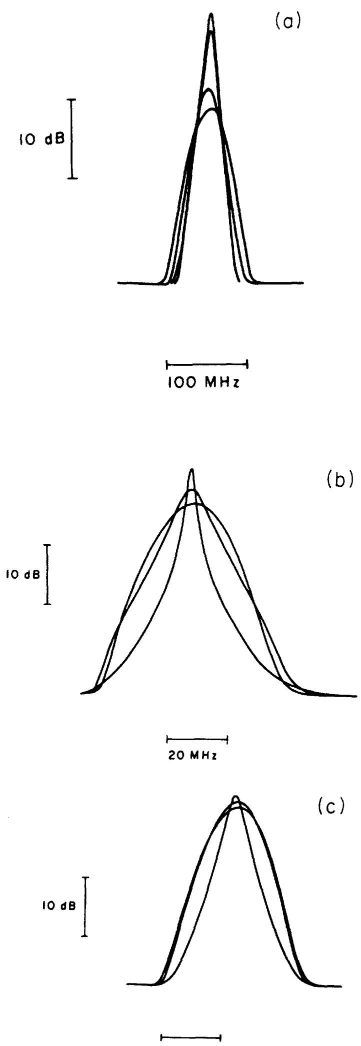

FIG. 6. Examples of laser power spectra (logarithmic plot) (a) $B=90$ MHz, $DV_{\rm rms}=7.9$, 18, 32, and 74 MHz (narrowest to widest). (b) $DV_{\rm rms}=7.9$ MHz, $B=90$, 27, and 10 MHz (narrowest to widest). (c) $DV_{\rm rms}=18$ MHz; $B=90$, 27, and 10 MHz (narrowest to widest).

V. CONCLUSION

We have succeeded in superimposing frequency fluctuations onto a laser beam in order to modify the bandwidth and band shape. Future improvements include methods of increasing the frequency response of the modulator, and of increasing the rate at which the frequency fluctuates. Modulation schemes employing electro-optic devices are also being considered.

ACKNOWLEDGMENTS

We gratefully acknowledge helpful discussions and ideas from J. Hall, L. Hollberg, S. Lissauer, and F. M. Pipkin, help with the computations from C. V. Kunasz, and technical assistance from D. Smith. This work was supported by the U. S. Department of Energy, Office of Basic Energy Sciences.

APPENDIX A

We outline here the evaluation of the term $\langle \exp\{i[\phi(t)-\phi(t+\tau)]\}\rangle$, leading to Eq. (3). The procedure involves the series expansion of the exponential

$$\langle \exp\{i[\phi(t)-\phi(t+\tau)]\}\rangle = \sum_{n=0}^{\infty} \frac{\langle \{i[\phi(t)-\phi(t+\tau)]\}^n\rangle}{n!} .$$

The Gaussian moment theorem[5] states that the odd moments of a Gaussian process vanish, and that the even moments are related to the second-order moment by the relation $\langle A^{2n}\rangle = [(2n!/2^n n!]\langle A^2\rangle^n$. This leads to

$$\langle \exp\{i[\phi(t)-\phi(t+\tau)]\}\rangle = \sum_{n=0}^{\infty} \frac{(i)^{2n}\langle [\phi(t)-\phi(t+\tau)]^{2n}\rangle}{(2n)!} = \sum_{n=0}^{\infty} \frac{(-1)^n \frac{(2n)!}{2^n n!}\langle [(\phi(t)-\phi(t+\tau)]^2\}\rangle^n}{(2n)!} .$$

Rearranging, and contracting the series back into an exponential, we obtain the desired result, which is used in Eq. (3)

$$\langle \exp\{i[\phi(t)-\phi(t+\tau)]\}\rangle = \sum_{n=0}^{\infty} \frac{[-\frac{1}{2}\langle (\phi(t)-\phi(t+\tau)]^2\rangle]^n}{n!} = \exp\{-\tfrac{1}{2}\langle [\phi(t)-\phi(t+\tau)]^2\rangle\} .$$

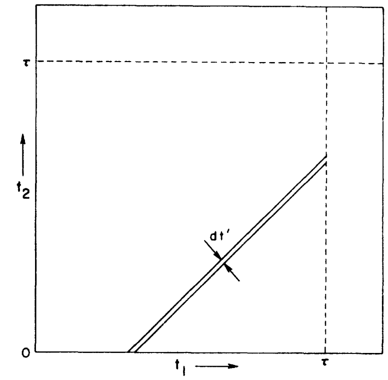

FIG. 7. Geometrical figure showing limits of integration over the differential element dt', leading to Eq. (B1).

APPENDIX B

We explain the last step in the derivation of Eq. (4), the evaluation of $\langle [\phi(t)-\phi(t+\tau)]^2\rangle$. Since $V(t)$ is a stationary process, the autocorrelation function $R_V(t_1,t_2) = \langle V(t_1)V(t_2)\rangle$ depends only upon the difference t_1-t_2, and is denoted $R_V(t_1-t_2)$. The double integral of a function which depends only on the difference between the two variables can be reduced to a single integral with the help of Fig. 7. We want to integrate $R_V(t_1-t_2)$ over the area shown, where $R_V(t_1-t_2)$ is constant over the diagonal strip. The strip is of length

$$\sqrt{2}(\tau-t_1) = 2(\tau/\sqrt{2}-t') ,$$

and of width dt', where $t'=(t_1-t_2)/\sqrt{2}$ and where t' is the new integration variable which varies from $-\tau/\sqrt{2}$ to $\tau/\sqrt{2}$ in a direction normal to the diagonal strip. Therefore

$$\int_0^\tau \int_0^\tau R_V(t_2-t_1)dt_1 dt_2 = 2\int_0^{\tau\sqrt{2}} dt' R_V(\sqrt{2}t')2\left[\frac{\tau}{\sqrt{2}}-t'\right]$$

where the factor 2 outside the integral is due to the integral extending over only one-half the area. Substituting $\sqrt{2}t' \rightarrow t$, we find that the integral is simply

$$\int_0^\tau \int_0^\tau \langle V(t_1)V(t_2)\rangle dt_1 dt_2 = 2\int_0^\tau dt\, R_V(t)(\tau-t) . \quad \text{(B1)}$$

*Quantum Physics Division, National Bureau of Standards.

[1]S. N. Dixit, P. Zoller, and P. Lambropoulos, Phys. Rev. A 21, 1289 (1980); J. J. Yeh and J. H. Eberly, *ibid.* 24, 888 (1981).

[2]G. S. Agarwal, Phys. Rev. A 18, 1490 (1978); K. I. Osman and S. Swain, J. Phys. B 13, 2397 (1980).

[3]S. A. Akhmanov, Yu. E. D'yakov, and L. I. Pavlov, Zh. Eksp. Teor. Fiz. 66, 520 (1974) [Sov. Phys.—JETP 39, 249 (1974)]; B. R. Marx, J. Simons, and L. Allen, J. Phys. B 11, L273 (1978); P. Agostini, A. T. Georges, S. E. Wheatly, P. Lambropoulos, and M. D. Levenson, *ibid.* 11, 1733 (1978); and P. B. Hogan, S. J. Smith, A. T. Georges, and P. Lambropoulos, Phys. Rev. Lett. 41, 229 (1978); D. E. Nitz, A. V. Smith, M. D. Levenson, and S. J. Smith, Phys. Rev. A 24, 288 (1981); F. Rohart and B. Macke, Appl. Phys. B 26, 23 (1981).

[4]D. Middleton, Philos. Mag. 42, 689 (1951). This work is reviewed in Ref. 5.

[5]D. Middleton, *An Introduction to Statistical Communication Theory* (McGraw-Hill, New York, 1960).

[6]J. L. Stewart, Proc. IRE 42, 1539 (1954).